

1 **Coarse particulate matter air quality in East Asia:**
2 **implications for fine particulate nitrate**

3 Shixian Zhai^{1,*}, Daniel J. Jacob¹, Drew C. Pendergrass¹, Nadia K. Colombi², Viral Shah¹,
4 Laura Hyesung Yang¹, Qiang Zhang³, Shuxiao Wang⁴, Hwajin Kim⁵, Yele Sun⁶, Jin-Soo
5 Choi⁷, Jin-Soo Park⁷, Gan Luo⁸, Fangqun Yu⁸, Jung-Hun Woo⁹, Younha Kim¹⁰, Jack E.
6 Dibb¹¹, Taehyoung Lee¹², Jin-Seok Han¹³, Bruce E. Anderson¹⁴, Ke Li¹⁵, Hong Liao¹⁵

7
8 ¹ John A. Paulson School of Engineering and Applied Sciences, Harvard University, Cambridge, MA 02138

9 ² Department of Earth and Planetary Science, Harvard University, Cambridge, MA 02138, USA

10 ³ Department of Earth System Science, Tsinghua University, Beijing 100084, China

11 ⁴ State Key Joint Laboratory of Environmental Simulation and Pollution Control, School of Environment,
12 Tsinghua University, Beijing 100084, China

13 ⁵ Department of Environmental Health Sciences, Graduate School of Public Health, Seoul National
14 University, Seoul 08826, South Korea

15 ⁶ State Key Laboratory of Atmospheric Boundary Layer Physics and Atmospheric Chemistry, Institute of
16 Atmospheric Physics, Chinese Academy of Sciences, Beijing 100029, China

17 ⁷ Air Quality Research Division, National Institute of Environmental Research, Incheon 22689, Republic of
18 Korea

19 ⁸ Atmospheric Sciences Research Center, University at Albany, Albany, NY 12226, USA

20 ⁹ Department of Civil and Environmental Engineering, Konkuk University, Seoul 05029, South Korea

21 ¹⁰ International Institute for Applied Systems Analysis (IIASA), Laxenburg 2361, Austria

22 ¹¹ Institute for the Study of Earth, Oceans, and Space, University of New Hampshire, Durham, NH 03824

23 ¹² Department of Environmental Science, Hankuk University of Foreign Studies, Yongin 449791, South
24 Korea

25 ¹³ Department of Environmental and Energy Engineering, Anyang University, Anyang 14028, South Korea

26 ¹⁴ NASA Langley Research Center, Hampton, VA 23681, USA

27 ¹⁵ Jiangsu Key Laboratory of Atmospheric Environment Monitoring and Pollution Control, Collaborative
28 Innovation Center of Atmospheric Environment and Equipment Technology, School of Environmental
29 Science and Engineering, Nanjing University of Information Science and Technology, Nanjing 210044,
30 China

31 *Correspondence to:* Shixian Zhai (zhaisx@g.harvard.edu)

32

33 **Abstract.** Air quality network data in China and South Korea show very high year-round mass
34 concentrations of coarse particulate matter (PM), as inferred by difference between PM_{10} and $PM_{2.5}$. Coarse
35 PM concentrations in 2015 averaged $52 \mu\text{g m}^{-3}$ in the North China Plain (NCP) and $23 \mu\text{g m}^{-3}$ in the Seoul
36 Metropolitan Area (SMA), contributing nearly half of PM_{10} . Strong daily correlations between coarse PM
37 and carbon monoxide imply a dominant source from anthropogenic fugitive dust. Coarse PM
38 concentrations in the NCP and the SMA decreased by 21% from 2015 to 2019 and further dropped abruptly
39 in 2020 due to COVID-19 reductions in construction and vehicle traffic. Anthropogenic coarse PM is
40 generally not included in air quality models but scavenges nitric acid to suppress the formation of fine
41 particulate nitrate, a major contributor to $PM_{2.5}$ pollution. GEOS-Chem model simulation of surface and
42 aircraft observations from the KORUS-AQ campaign over the SMA in May-June 2016 shows that
43 consideration of anthropogenic coarse PM largely resolves the previous model overestimate of fine
44 particulate nitrate. The effect is smaller in the NCP which has a larger excess of ammonia. Model
45 sensitivity simulations for 2015-2019 show that decreasing anthropogenic coarse PM directly increases
46 $PM_{2.5}$ nitrate in summer, offsetting 80% the effect of nitrogen oxide and ammonia emission controls, while
47 in winter the presence of coarse PM increases the sensitivity of $PM_{2.5}$ nitrate to ammonia and sulfur dioxide
48 emissions. Decreasing coarse PM helps to explain the lack of decrease in wintertime $PM_{2.5}$ nitrate observed
49 in the NCP and the SMA over the 2015-2021 period despite decreases in nitrogen oxide and ammonia
50 emissions. Continuing decrease of fugitive dust pollution means that more stringent nitrogen oxide and
51 ammonia emission controls will be required to successfully decrease $PM_{2.5}$ nitrate.

52 **1. Introduction**

53 Coarse particulate matter (coarse PM; particulate matter between $2.5 \mu\text{m}$ and $10 \mu\text{m}$ aerodynamic diameter)
54 is a severe air pollution problem in East Asia, contributing a particle mass comparable to fine particulate
55 matter ($PM_{2.5}$) and thus about half of PM_{10} (Chen et al., 2019; Lee et al., 2015; Qiu et al., 2014; Wang et al.,
56 2018a). It is mainly fugitive mineral dust, with contributions from both natural desert dust and
57 anthropogenic sources including on-road traffic, construction, and agriculture (Wu et al., 2016; Zhao et al.,
58 2017; Liu et al., 2021; Khatra, 2020). Atmospheric chemistry models used in air quality applications
59 generally do not include anthropogenic fugitive dust, due to the lack of available emission inventories
60 except for a few urban areas (Li et al., 2021a; Li et al., 2021b; Li et al., 2021c). Aside from its direct
61 interest as an air pollutant, coarse PM can suppress $PM_{2.5}$ by heterogeneously taking up acids (HNO_3 , SO_2 ,
62 and H_2SO_4) that would otherwise lead to $PM_{2.5}$ formation. This uptake has been observed for natural dust
63 events (Wang et al., 2017; Heim et al., 2020; Wang et al., 2018b; Park et al., 2004; Stone et al., 2011), but
64 the more ubiquitous effect from anthropogenic dust has received little study (Kakavas and Pandis, 2021;
65 Hodzic et al., 2006). With increasingly stringent control measures to decrease fugitive dust air pollution in
66 East Asia (Chinese State Council, 2019; Noh et al., 2018; Wu et al., 2016; Xing et al., 2018), it is important
67 to better understand the impact on $PM_{2.5}$ air quality.

68 A specific issue is the effect of anthropogenic dust on PM_{2.5} nitrate. Nitrate is a major component of
69 PM_{2.5} in urban regions of East Asia including the North China Plain (NCP) (Li et al., 2019; Zhai et al.,
70 2021a) and the Seoul Metropolitan Area (SMA) (Jeong et al., 2022; Kim et al., 2020), and it can dominate
71 haze pollution events in both regions (Fu et al., 2020; Li et al., 2018; Xu et al., 2019; Kim et al., 2017; Kim
72 et al., 2020). PM_{2.5} nitrate over North China in winter has not decreased in recent years despite reductions
73 in emissions of the precursor nitrogen oxides (NO_x ≡ NO + NO₂) (Zhai et al., 2021a; Fu et al., 2020) from
74 fossil fuel combustion. This has been attributed to limitation by ammonia (NH₃) emissions, since PM_{2.5}
75 nitrate is mainly present as ammonium nitrate (Zhai et al., 2021a). Decreasing coarse PM emissions is
76 another possible explanation as it would allow more HNO₃ to be available for PM_{2.5} nitrate formation, and
77 it could also shift PM_{2.5} nitrate formation to be more NH₃-limited. Better understanding this sensitivity of
78 PM_{2.5} nitrate to coarse PM is of crucial importance because of recent efforts by the Chinese government to
79 decrease NH₃ emissions (Liao et al., 2022), which are mainly from agriculture with additional urban
80 contributions from vehicle, industrial, and waste disposal sources (Mgelwa et al., 2022).

81 In this work, we show that coarse PM over the NCP and the SMA is mainly anthropogenic and decreased
82 by 21% during the 2015-2019 period. We find that accounting for this anthropogenic coarse PM in the
83 GEOS-Chem atmospheric chemistry model greatly improves the ability of the model to simulate PM_{2.5}
84 nitrate during the KORUS-AQ aircraft campaign over Korea where previous GEOS-Chem simulations
85 found a large overestimate (Travis et al., 2022; Zhai et al., 2021b). From there we examine the implications
86 for the effects of emission controls on long-term trends of PM_{2.5} nitrate in China and South Korea.

87 2. Coarse PM in China and South Korea

88 Figure 1 shows the annual mean concentrations of coarse PM in 2015, 2019, and 2020 measured at air
89 quality networks in China and South Korea as the PM₁₀ – PM_{2.5} difference. Data for China are from the
90 Ministry of Ecology and Environment (MEE) network (<http://www.quotsoft.net/air/>) and data for South
91 Korea are from the AirKorea network (<https://www.airkorea.or.kr>). We remove spurious data when PM_{2.5} is
92 higher than PM₁₀, which account for 1.7% and 0.2% of the dataset respectively in China and South Korea.

93 We see from Fig. 1 that coarse PM concentrations in China and South Korea are highest in the NCP and
94 the SMA, respectively, indicating a dominant urban anthropogenic origin. Coarse PM in year 2015
95 averaged 52 μg m⁻³ in the NCP and 23 μg m⁻³ in the SMA, contributing nearly half of total PM₁₀ (120 μg m⁻³
96 in the NCP and 50 μg m⁻³ in the SMA). National air quality standards for annual mean PM₁₀ are 70 μg m⁻³
97 in China (urban) and 50 μg m⁻³ in South Korea, well above the World Health Organization (WHO)
98 recommended annual standard of 15 μg m⁻³. Coarse PM decreased by 21% in both the NCP and the SMA
99 from 2015 to 2019, reflecting emission controls on fugitive dust (Chinese State Council, 2013, 2018; Noh
100 et al., 2018; Wu et al., 2016), and further decreased strongly in 2020 because of COVID-19 restrictions on

101 traffic and construction. The COVID-19 impact is evident in China by comparing concentrations before
102 and after the sharp January 24, 2020 lockdown (Fig. 2).

103 Figure 3 shows further evidence of the dominant anthropogenic contribution to coarse PM as the daily
104 correlation with carbon monoxide (CO) in 2015. CO is emitted by incomplete combustion and is a tracer of
105 urban influence. We find strong correlations between coarse PM and CO with consistent slopes except in
106 spring, which features high coarse PM outliers attributable to desert dust events (Heim et al., 2020; Shao
107 and Dong, 2006). Similar correlations to 2015 are found in other years (Fig. S1). The desert dust events
108 drive the seasonal maximum of coarse PM in Fig. 1h.

109 **3. Effect of anthropogenic coarse PM on fine particulate nitrate during KORUS-AQ**

110 We simulated the effect of anthropogenic coarse PM on PM_{2.5} nitrate using the GEOS-Chem model and
111 evaluated the model with observations from the KORUS-AQ aircraft campaign over South Korea in May-
112 June 2016 (Crawford et al., 2021). KORUS-AQ offers a unique data set of detailed aerosol and gas-phase
113 composition over East Asia. Previous GEOS-Chem simulations showed a large overestimate of fine
114 particulate nitrate and a large underestimate of coarse PM (Travis et al., 2022; Zhai et al., 2021b).
115 Particulate nitrate concentrations were measured during KORUS-AQ at the Korea Institute of Science and
116 Technology (KIST) surface site and on the aircraft by Aerosol Mass Spectrometers (AMS) with size cut of
117 1 μm diameter (PM₁ nitrate) (Kim et al., 2017; Kim et al., 2018). The AMS only detects non-refractory
118 nitrate, taken here to be ammonium nitrate (Fig. S2). Total particulate nitrate with size cut of 4 μm diameter
119 (PM₄ nitrate) was also sampled on the aircraft by the Soluble Acidic Gases and Aerosol (SAGA) instrument
120 (Dibb et al., 2003; McNaughton et al., 2007). Additional measurements on the aircraft included HNO₃
121 concentrations with a Chemical Ionization Time of Flight Mass Spectrometer (CIT-ToF-CIMS), and
122 aerosol size distributions including coarse PM with a DMT CPSPD Probe. We focus on the observations
123 over the SMA and exclude observations from two process-directed flights (RF7 and RF8) and the Daesan
124 power plant plume following Park et al. (2021).

125 We use GEOS-Chem version 13.0.2 (<https://zenodo.org/record/4681204>) in a nested-grid simulation
126 over East Asia (100 - 150° E, 20 - 50° N) with a horizontal resolution of 0.5° \times 0.625°. The model simulates
127 detailed oxidant-aerosol chemistry relevant to PM_{2.5} nitrate formation (Zhai et al., 2021a) and is driven by
128 meteorological data from the NASA Modern-Era Retrospective Analysis for Research and Applications,
129 Version 2 (MERRA-2). Formation of semi-volatile ammonium nitrate aerosol is governed by ISORROPIA
130 version 2.2 thermodynamics (Fountoukis and Nenes, 2007). Dry deposition of gases and particles follows a
131 standard resistance-in-series scheme (Wesely, 1989). Wet deposition of gases and particles includes
132 contributions from rainout, washout, and scavenging in convective updrafts (Liu et al., 2001; Luo et al.,
133 2019). The model includes reactive uptake of HNO₃ on dust limited by dust alkalinity and mass transfer
134 (Fairlie et al., 2010), assuming 7.1 % Ca²⁺ and 1.1% Mg²⁺ as carbonates per mass in emitted dust (Shah et

135 al., 2020a; Tang and Han, 2017; Zhang et al., 2014). The relative humidity (RH)-dependent reactive uptake
136 coefficient (γ) of HNO_3 is based on laboratory studies (Liu et al., 2008; Huynh and McNeill, 2020) and
137 observations during natural dust events in Beijing (Tian et al., 2021; Wang et al., 2017), and increases from
138 0.06 to 0.21 as RH increases from 40% to 80%. Monthly anthropogenic emissions for China are from the
139 Multi-resolution Emission Inventory for China (MEIC) (Zheng et al., 2018; Zheng et al., 2021a; Zheng et
140 al., 2021b), and emissions for other Asian countries including South Korea are from the KORUSv5
141 inventory (Woo et al., 2020). Fine anthropogenic mineral dust emissions from combustion and industrial
142 sources (ash) are derived from the MEIC and KORUSv5 inventories as the residual of anthropogenic
143 primary $\text{PM}_{2.5}$ emissions after excluding primary organic aerosol, black carbon, and primary sulfate (Philip
144 et al., 2017).

145 We compare the results from the standard model as described above to a simulation where we add
146 anthropogenic coarse PM by using 24-hour average observed coarse PM concentrations from the air quality
147 networks (Fig. 1) as boundary conditions at the lowest model level. For this purpose, we linearly interpolate
148 the daily mean coarse PM data from the network to the GEOS-Chem model horizontal grid and apply them
149 to the coarse dust GEOS-Chem model component with an effective diameter of 4.8 μm . This concentration
150 boundary condition in the lowest model level serves as an implicit source and defines the vertical
151 concentration profile. The resulting vertical profiles of coarse PM in GEOS-Chem over South Korea are
152 consistent with KORUS-AQ aircraft observations (Fig. S3). Anthropogenic coarse PM is assumed to be
153 mainly fugitive dust with the same alkalinity properties as natural dust (Zhang et al., 2014; Tang and Han,
154 2017).

155 Figure 4 compares GEOS-Chem to the KORUS-AQ observations including median diurnal PM_1 nitrate
156 at the KIST site and median aircraft vertical profiles over the SMA. The model is sampled along the aircraft
157 flight tracks at the times of the observations, all in daytime. PM_{1-4} nitrate is derived as the difference
158 between SAGA PM_4 nitrate and AMS PM_1 nitrate. Here we take ammonium nitrate in the model for
159 comparison to PM_1 observations, and size-resolved dust nitrate for comparison to PM_{1-4} observations. In
160 this way, any dust-associated refractory PM_1 nitrate is included in the PM_{1-4} profiles, for both observations
161 and the GEOS-Chem model. Such classification does not allow for supermicron ammonium nitrate, but
162 KORUS-AQ observations found ammonium nitrate to be mainly submicron (Kim et al., 2018). GEOS-
163 Chem results are shown both for the standard model (not including anthropogenic coarse PM) and with the
164 addition of anthropogenic coarse PM. In both simulations, we adjusted the diurnal variation of NH_3
165 emission to match the NH_3 observations made at the Olympic Park site, 7 km southeast of KIST (Fig. S4).

166 The standard GEOS-Chem simulation without anthropogenic fugitive dust overestimates daytime PM_1
167 nitrate (aircraft and surface) by about a factor of two while underestimating PM_{1-4} nitrate by about a factor
168 of two (Fig. 4a, b, and c). Coarse PM in the standard simulation (from natural dust and sea salt) is near

169 zero, in contrast to observations (Fig. 4d). Adding anthropogenic coarse PM to the model corrects this bias
170 and further corrects the PM₁ and PM₁₋₄ nitrate biases by providing an added sink for HNO₃. We find that
171 anthropogenic coarse PM takes up HNO₃ three times faster than dry deposition and that this uptake is
172 limited by mass-transfer rather than alkalinity (only 60-70% of the coarse dust alkalinity in surface air is
173 neutralized on average). The shift from PM₁ to PM₁₋₄ nitrate is consistent with the uptake of HNO₃ by
174 coarse PM, with some of this uptake in the model taking place on dust coarser than 4 μm and so not
175 observed by PM₁₋₄ nitrate. Half of the model overestimate of HNO₃ is corrected (Fig. 4e), with the
176 remainder possibly due to an underestimate of HNO₃ deposition velocity (Travis et al., 2022). The model
177 overestimates nighttime nitrate in surface air at the KIST site, even with anthropogenic coarse PM. This
178 nighttime nitrate in the model is driven by heterogeneous NO₂ and N₂O₅ chemistry under stratified
179 conditions, which could be subject to large local errors (Travis et al., 2022).

180 We also examined the effect of anthropogenic coarse PM on PM_{2.5} nitrate concentrations in the NCP.
181 PM_{2.5} nitrate observations in NCP are mostly filter-collected bulk PM_{2.5} nitrate, which could be biased low
182 in summer due to volatilization (Chow et al., 2005). Previous evaluation of GEOS-Chem with 2013 and
183 2015 PM_{2.5} nitrate observations across China in summer and winter found no significant bias in 2015 or
184 winter 2013 but an overestimate in summer 2013 (Zhai et al., 2021a). That simulation did not include
185 HNO₃ uptake by dust (natural or anthropogenic). We find here that including HNO₃ uptake by fine (PM_{2.5})
186 dust has little effect on total PM_{2.5} nitrate but partitions 10% of ammonium nitrate mass to fine dust nitrate
187 in winter and 23% in summer (Fig. S5). Adding anthropogenic coarse PM in GEOS-Chem decreases
188 modeled ammonium nitrate in the NCP by 10-20% in winter and by 25-30% in summer, a relatively more
189 modest effect than over the SMA because of larger excess of NH₃. The comparison with PM_{2.5} nitrate
190 observations here indicates that fine dust associated nitrate should be considered when comparing modeled
191 particle nitrate to bulk PM_{2.5} nitrate data.

192 **4. Implications for long-term trends of PM_{2.5} nitrate and responses to emission controls**

193 There are to our knowledge no continuous long-term records of PM_{2.5} nitrate concentrations in China or
194 South Korea. Figure 5 shows a multi-year compilation of winter and summer mean PM₁ and PM_{2.5} nitrate
195 observations from individual field campaigns in Beijing and Seoul over 2015-2021 (Table S1). We find no
196 significant trends in winter, consistent with previous studies in the NCP that examined shorter periods (Fu
197 et al., 2020). In summer, observations tend to show a decrease over the period but with large interannual
198 variations driven by meteorology (Li et al., 2018; Zhai et al., 2021a).

199 Changes in anthropogenic emissions of NO_x, SO₂, NH₃, PM_{2.5}, and coarse PM could all affect PM_{2.5}
200 nitrate, and we used GEOS-Chem to investigate these effects for the 2015-2019 period. The Multi-
201 resolution Emission Inventory for China (MEIC) reports that NO_x emissions in the NCP decreased by 11%
202 from 2015 to 2019, SO₂ emissions decreased by 54%, and primary PM_{2.5} from combustion decreased by

203 35% (Zheng et al., 2021a). This primary PM_{2.5} includes a 40% contribution from mineral ash that we treat
204 as anthropogenic fine dust and decreased by 27% from 2015 to 2019. The MEIC also reports a 15%
205 decrease of NH₃ emissions over China from 2015 to 2019 (19% for the NCP), while the PKU-NH₃
206 emission inventory reports a 6% decrease over China from 2015 to 2018 (Liao et al., 2022). Observations
207 of surface NO₂ and SO₂ over the SMA imply a 22% decrease of NO_x emissions and a 40% decrease of SO₂
208 emissions from 2015 to 2019 (Bae et al., 2021; Colombi et al., 2022). Coarse PM decreased by 33% over
209 the NCP and by 31% over SMA during the same period (considering winter and summer data only).

210 Figure 6 shows the resulting emission-driven changes of PM_{2.5} nitrate over the NCP and SMA from 2015
211 to 2019 as simulated by GEOS-Chem in sensitivity simulations applying either 2015 or 2019 emissions to
212 the same meteorological year (2019), and with or without anthropogenic coarse PM. The sum of changes
213 driven by individual emission changes amounts to the total emission-driven net change. Sensitivities to
214 NH₃ and primary PM_{2.5} emissions in the SMA are solely driven by emission trends in China since we
215 assume no emission trends for these species in South Korea.

216 The model reproduces the lack of trend in winter and the decreasing trend in summer seen in the
217 observations for both the NCP and SMA. The lack of trend in winter reflects offsetting influences from
218 decreasing NO_x, NH₃, and primary PM_{2.5} emissions on the one hand, and decreasing SO₂ and coarse PM
219 emissions on the other hand. Decreasing SO₂ increases the availability of NH₃ for nitrate formation (Fu et
220 al., 2020; Zhai et al., 2021a). Decreasing primary PM_{2.5} reduces the aerosol volume available for
221 heterogeneous conversion of NO_x to HNO₃ (Shah et al., 2020b). Decreasing coarse PM has relatively little
222 direct effect on PM_{2.5} nitrate in winter in the NCP because abundant atmospheric NH₃ combined with low
223 temperatures drives HNO₃ near-quantitatively to ammonium-nitrate particles, and subsequent mass transfer
224 of HNO₃ from ammonium nitrate to coarse PM is very slow because of the weak HNO₃ partial pressure
225 (Wexler and Seinfeld, 1992). The decrease of coarse PM still quantitatively offsets the benefit from NO_x
226 emission controls, which has been the main vehicle for controlling PM_{2.5} nitrate. Consideration of coarse
227 PM in the model further increases the sensitivity of PM_{2.5} nitrate to NH₃ and SO₂ emissions respectively by
228 30% and 46%. This is because coarse PM provides an additional sink for the small fraction of HNO₃ that
229 remains in the gas phase, which increases the sensitivity of the atmospheric lifetime of total nitrate
230 (ammonium nitrate + HNO₃) to changes in NH₃ or SO₂ emissions (Zhai et al., 2021a).

231 In summer, we find that the decrease in coarse PM over the 2015-2019 period directly cancels half of the
232 benefit from decreasing NO_x, SO₂, NH₃, and primary PM_{2.5} emissions in the NCP, with less effect in the
233 SMA. Over the NCP, the decrease of coarse PM offsets 80% of the benefits from NO_x and NH₃ emission
234 controls. Unlike in winter, decreasing SO₂ suppresses nitrate formation by decreasing the aerosol liquid
235 water content (Stelson and Seinfeld, 1982). The effect of decreasing coarse PM emissions in summer is
236 larger than in winter because warmer temperatures allow more HNO₃ to remain in the gas phase under

237 $\text{NH}_3\text{-HNO}_3\text{-H}_2\text{SO}_4$ thermodynamics and thus be scavenged by coarse PM.

238 **5. Conclusions**

239 Coarse PM (PM_{10} - $\text{PM}_{2.5}$) in urban areas of China and South Korea is very high year-round and is mainly
240 of anthropogenic origin as fugitive dust except for natural desert dust events in spring. Annual mean coarse
241 PM concentrations decreased by 21% from 2015 to 2019 in both the North China Plain (NCP) and the
242 Seoul Metropolitan Area (SMA), with steeper decreases in 2020 because of COVID-19 restrictions on
243 traffic and construction. Considering only winter and summer when the influence of natural dust is small,
244 we find that anthropogenic fugitive dust emissions decreased by about 30% from 2015 to 2019 in both the
245 NCP and the SMA.

246 Anthropogenic coarse PM is of direct air quality concern because it accounts for about half of total PM_{10}
247 in the NCP and the SMA, but it also takes up HNO_3 effectively and can thus suppress formation of fine
248 particulate nitrate which is a major component of $\text{PM}_{2.5}$ pollution. Comparison of GEOS-Chem model
249 simulations to surface and aircraft observations from the KORUS-AQ campaign over the SMA in May-
250 June 2016 shows that accounting for anthropogenic coarse PM largely corrects previous model
251 overestimates of fine particulate nitrate.

252 Decrease in anthropogenic coarse PM emissions to improve PM_{10} air quality could have the unintended
253 consequence of increasing $\text{PM}_{2.5}$ nitrate, offsetting the gains from decreases in NO_x and NH_3 emissions.
254 Compilation of 2015-2021 observations of fine particulate nitrate in Beijing and Seoul suggests little trend
255 in winter and a decrease in summer, consistent with GEOS-Chem. Decreasing coarse PM in the model in
256 winter offsets the benefit of decreasing NO_x emissions, and coarse PM further increases the sensitivity of
257 $\text{PM}_{2.5}$ nitrate to changes in NH_3 and SO_2 emissions by affecting the lifetime of total inorganic nitrate
258 (ammonium nitrate + HNO_3). In summer, decreasing coarse PM in the NCP offsets 80% of the $\text{PM}_{2.5}$ nitrate
259 benefit of decreasing NO_x and NH_3 emissions. As coarse PM continues to decrease in response to fugitive
260 dust pollution control, there is a greater need to reduce NH_3 and NO_x emissions in order to decrease fine
261 particulate nitrate air pollution in East Asia.

262

263 *Data availability.* $\text{PM}_{2.5}$, PM_{10} , and CO data over China are from <http://www.quotsoft.net/air/>, over South
264 Korea are from https://www.airkorea.or.kr/web/last_amb_hour_data?pMENU_NO=123. Surface and
265 aircraft data during KORUS-AQ are from <https://doi.org/10.5067/Suborbital/KORUSAQ/DATA01>. Multi-
266 year compilation of winter and summer mean PM_1 and $\text{PM}_{2.5}$ nitrate are provided in Table S1.

267

268 *Supplement.* The supplement related to this article is uploaded at submission.

269

270 *Author Contributions.* S.Z. and D.J.J. designed the research. S.Z. performed the research. D.C.P., N.K.C.,
271 V.S., L.H.Y., and H.L. helped with data analysis and results interpretation. Q.Z. provided the MEIC
272 emission inventory. S.W., H.K., Y.S., J.S.C, J.S.P., J.E.D., T.L., J.S.H, and B.E.A provided observation
273 data. J.H.W. and Y.K. provided the KORUSv5 emission inventory. G.L., F.Y., and K.L. helped with model
274 simulations. S.Z. and D.J.J wrote the paper with input from all other authors.

275

276 *Competing Interests.* The authors declare no competing interests.

277

278 *Financial support.* This work was funded by the Harvard–NUIST Joint Laboratory for Air Quality and
279 Climate (JLAQC) and the Samsung Advanced Institute of Technology.

280

281 *Acknowledgments.* We thank Bo Zheng (Tsinghua Shenzhen International Graduate School, Tsinghua
282 University) for processing the MEIC emission inventory. We thank Paul O. Wennberg, Michelle J. Kim,
283 Alexander P. Teng, and John D. Crouse from the California Institute of Technology for their contributions
284 to HNO₃ measurements during KORUS-AQ.

285

286 **References**

287 Bae, M., Kim, B.-U., Kim, H. C., Kim, J., and Kim, S.: Role of emissions and meteorology in the
288 recent PM_{2.5} changes in China and South Korea from 2015 to 2018, *Environ. Pollut.*, 270,
289 116233, <https://doi.org/10.1016/j.envpol.2020.116233>, 2021.

290 Chen, R., Yin, P., Meng, X., Wang, L., Liu, C., Niu, Y., Liu, Y., Liu, J., Qi, J., You, J., Kan, H.,
291 and Zhou, M.: Associations between Coarse Particulate Matter Air Pollution and Cause-
292 Specific Mortality: A Nationwide Analysis in 272 Chinese Cities, *Environ. Health Perspect.*,
293 127, 017008, <https://doi.org/10.1289/EHP2711>, 2019.

294 Chow, J. C., Watson, J. G., Lowenthal, D. H., and Magliano, K. L.: Loss of PM_{2.5} nitrate from
295 filter samples in central California, *J. Air Waste Manag. Assoc.*, 55, 1158-1168,
296 <https://doi.org/10.1080/10473289.2005.10464704>, 2005.

297 Colombi, N. K., Jacob, D. J., Yang, L. H., Zhai, S., Shah, V., Grange, S. K., Yantosca, R. M.,
298 Kim, S., and Liao, H.: Why is ozone in South Korea and the Seoul Metropolitan Area so
299 high and increasing?, *EGUsphere*, 2022, 1-21, 10.5194/egusphere-2022-1366, 2022.

300 Chinese State Council: Action Plan on Prevention and Control of Air Pollution,
301 http://www.gov.cn/zwggk/2013-09/12/content_2486773.htm (last access: December 18
302 2022), 2013 (in Chinese).

303 Chinese State Council: Three-year Action Plan for Protecting Blue Sky,
304 http://www.gov.cn/zhengce/content/2018-07/03/content_5303158.htm (last access:
305 December 18 2022), 2018 (in Chinese).

306 Chinese State Council: Beijing has set up more than 1,000 sites to monitor dust,
307 http://www.gov.cn/xinwen/2019-04/16/content_5383488.htm (last access: December 18
308 2022), 2019 (in Chinese).

309 Crawford, J. H., Ahn, J.-Y., Al-Saadi, J., Chang, L., Emmons, L. K., Kim, J., Lee, G., Park, J.-H.,
310 Park, R. J., Woo, J. H., Song, C.-K., Hong, J.-H., Hong, Y.-D., Lefer, B. L., Lee, M., Lee,
311 T., Kim, S., Min, K.-E., Yum, S. S., Shin, H. J., Kim, Y.-W., Choi, J.-S., Park, J.-S.,
312 Szykman, J. J., Long, R. W., Jordan, C. E., Simpson, I. J., Fried, A., Dibb, J. E., Cho, S., and
313 Kim, Y. P.: The Korea–United States Air Quality (KORUS-AQ) field study, *Elementa-Sci.*
314 *Anthrop.*, 9 (1), 1-27, <https://doi.org/10.1525/elementa.2020.00163>, 2021.

315 Dibb, J. E., Talbot, R. W., Scheuer, E. M., Seid, G., Avery, M. A., and Singh, H. B.: Aerosol
316 chemical composition in Asian continental outflow during the TRACE-P campaign:
317 Comparison with PEM-West B, *J. Geophys. Res. Atmos.*, 108, 8815,
318 <https://doi.org/10.1029/2002JD003111>, 2003.

319 Fairlie, T. D., Jacob, D. J., Dibb, J. E., Alexander, B., Avery, M. A., van Donkelaar, A., and
320 Zhang, L.: Impact of mineral dust on nitrate, sulfate, and ozone in transpacific Asian
321 pollution plumes, *Atmos. Chem. Phys.*, 10, 3999-4012, [https://doi.org/10.5194/acp-10-3999-](https://doi.org/10.5194/acp-10-3999-2010)
322 [2010](https://doi.org/10.5194/acp-10-3999-2010), 2010.

323 Fountoukis, C. and Nenes, A.: ISORROPIA II: a computationally efficient thermodynamic
324 equilibrium model for K^+ - Ca^{2+} - Mg^{2+} - NH_4^+ - Na^+ - SO_4^{2-} - NO_3^- - Cl^- - H_2O aerosols, *Atmos.*
325 *Chem. Phys.*, 7, 4639-4659, <https://doi.org/10.5194/acp-7-4639-2007>, 2007.

326 Fu, X., Wang, T., Gao, J., Wang, P., Liu, Y., Wang, S., Zhao, B., and Xue, L.: Persistent Heavy
327 Winter Nitrate Pollution Driven by Increased Photochemical Oxidants in Northern China,
328 *Environ. Sci. Technol.*, 54, 3881–3889, <https://doi.org/10.1021/acs.est.9b07248>, 2020.

329 Heim, E. W., Dibb, J., Scheuer, E., Jost, P. C., Nault, B. A., Jimenez, J. L., Peterson, D., Knote,
330 C., Fenn, M., Hair, J., Beyersdorf, A. J., Corr, C., and Anderson, B. E.: Asian dust observed
331 during KORUS-AQ facilitates the uptake and incorporation of soluble pollutants during
332 transport to South Korea, *Atmos. Environ.*, 224, 117305,
333 <https://doi.org/10.1016/j.atmosenv.2020.117305>, 2020.

334 Hodzic, A., Bessagnet, B., and Vautard, R.: A model evaluation of coarse-mode nitrate
335 heterogeneous formation on dust particles, *Atmos. Environ.*, 40, 4158-4171,
336 <https://doi.org/10.1016/j.atmosenv.2006.02.015>, 2006.

337 Huynh, H. N. and McNeill, V. F.: Heterogeneous Chemistry of $CaCO_3$ Aerosols with HNO_3 and
338 HCl , *J. Phys. Chem.*, 124, 3886-3895, <https://doi.org/10.1021/acs.jpca.9b11691>, 2020.

339 Jeong, J. I., Seo, J., and Park, R. J.: Compromised Improvement of Poor Visibility Due to PM
340 Chemical Composition Changes in South Korea, *Remote Sens.*, 14, 5310,
341 <https://doi.org/10.3390/rs14215310>, 2022.

342 Kakavas, S. and Pandis, S. N.: Effects of urban dust emissions on fine and coarse PM levels and
343 composition, *Atmos. Environ.*, 246, 118006,
344 <https://doi.org/10.1016/j.atmosenv.2020.118006>, 2021.

345 Katra, I.: Soil Erosion by Wind and Dust Emission in Semi-Arid Soils Due to Agricultural
346 Activities, *Agronomy*, 10 (1), 89, <https://doi.org/10.3390/agronomy10010089>, 2020.

347 Kim, H., Zhang, Q., and Heo, J.: Influence of intense secondary aerosol formation and long-range
348 transport on aerosol chemistry and properties in the Seoul Metropolitan Area during spring
349 time: results from KORUS-AQ, *Atmos. Chem. Phys.*, 18, 7149-7168,
350 <https://doi.org/10.5194/acp-18-7149-2018>, 2018.

351 Kim, H., Zhang, Q., and Sun, Y.: Measurement report: Characterization of severe spring haze
352 episodes and influences of long-range transport in the Seoul metropolitan area in March
353 2019, *Atmos. Chem. Phys.*, 20, 11527-11550, <https://doi.org/10.5194/acp-20-11527-2020>,
354 2020.

355 Kim, H., Zhang, Q., Bae, G. N., Kim, J. Y., and Lee, S. B.: Sources and atmospheric processing
356 of winter aerosols in Seoul, Korea: insights from real-time measurements using a high-
357 resolution aerosol mass spectrometer, *Atmos. Chem. Phys.*, 17, 2009-2033,
358 <https://doi.org/10.5194/acp-17-2009-2017>, 2017.

359 Lee, H., Honda, Y., Hashizume, M., Guo, Y. L., Wu, C.-F., Kan, H., Jung, K., Lim, Y.-H., Yi, S.,
360 and Kim, H.: Short-term exposure to fine and coarse particles and mortality: A multicity
361 time-series study in East Asia, *Environ. Pollut.*, 207, 43-51,
362 <https://doi.org/10.1016/j.envpol.2015.08.036>, 2015.

363 Li, H., Cheng, J., Zhang, Q., Zheng, B., Zhang, Y., Zheng, G., and He, K.: Rapid transition in
364 winter aerosol composition in Beijing from 2014 to 2017: response to clean air actions,
365 *Atmos. Chem. Phys.*, 19, 11485-11499, <https://doi.org/10.5194/acp-19-11485-2019>, 2019.

366 Li, H., Zhang, Q., Zheng, B., Chen, C., Wu, N., Guo, H., Zhang, Y., Zheng, Y., Li, X., and He,
367 K.: Nitrate-driven urban haze pollution during summertime over the North China Plain,
368 *Atmos. Chem. Phys.*, 18, 5293-5306, <https://doi.org/10.5194/acp-18-5293-2018>, 2018.

369 Li, T., Bi, X., Dai, Q., Wu, J., Zhang, Y., and Feng, Y.: Optimized approach for developing soil
370 fugitive dust emission inventory in "2+26" Chinese cities, *Environ. Pollut.*, 285, 117521,
371 <https://doi.org/10.1016/j.envpol.2021.117521>, 2021a.

372 Li, T., Dong, W., Dai, Q., Feng, Y., Bi, X., Zhang, Y., and Wu, J.: Application and validation of
373 the fugitive dust source emission inventory compilation method in Xiong'an New Area,
374 China, *Sci. Total Environ.*, 798, 149114, <https://doi.org/10.1016/j.scitotenv.2021.149114>,
375 2021b.

376 Li, T., Ma, S., Liang, W., Li, L., Dai, Q., Bi, X., Wu, J., Zhang, Y., and Feng, Y.: Application of
377 the high spatiotemporal resolution soil fugitive dust emission inventory compilation method
378 based on CAMx model, *Atmos. Res.*, 262, 105770,
379 <https://doi.org/10.1016/j.atmosres.2021.105770>, 2021c.

380 Liao, W., Liu, M., Huang, X., Wang, T., Xu, Z., Shang, F., Song, Y., Cai, X., Zhang, H., Kang,
381 L., and Zhu, T.: Estimation for ammonia emissions at county level in China from 2013 to
382 2018, *Sci. China Earth Sci.*, 65, 1116-1127, <https://doi.org/10.1007/s11430-021-9897-3>,
383 2022.

384 Liu, H., Jacob, D. J., Bey, I., and Yantosca, R. M.: Constraints from ^{210}Pb and ^7Be on wet
385 deposition and transport in a global three-dimensional chemical tracer model driven by
386 assimilated meteorological fields, *J. Geophys. Res. Atmos.*, 106, 12109-12128,
387 <https://doi.org/10.1029/2000JD900839>, 2001.

388 Liu, S., Xing, J., Sahu, S. K., Liu, X., Liu, S., Jiang, Y., Zhang, H., Li, S., Ding, D., Chang, X.,
389 and Wang, S.: Wind-blown dust and its impacts on particulate matter pollution in Northern
390 China: current and future scenarios, *Environ. Res. Lett.*, 16, 114041,
391 <http://dx.doi.org/10.1088/1748-9326/ac31ec>, 2021.

392 Liu, Y., Gibson, Cain, Wang, H., Grassian, and Laskin, A.: Kinetics of Heterogeneous Reaction
393 of CaCO_3 particles with Gaseous HNO_3 over a Wide Range of Humidity, *J. Phys. Chem. A*,
394 112, 1561-1571, <https://doi.org/10.1021/jp076169h>, 2008.

395 Luo, G., Yu, F., and Schwab, J.: Revised treatment of wet scavenging processes dramatically
396 improves GEOS-Chem 12.0.0 simulations of nitric acid, nitrate, and ammonium over the
397 United States, *Geosci. Model Dev.*, 12, 3439-3447 [https://doi.org/10.5194/gmd-12-3439-](https://doi.org/10.5194/gmd-12-3439-2019)
398 [2019](https://doi.org/10.5194/gmd-12-3439-2019), 2019.

399 McNaughton, C. S., Clarke, A. D., Howell, S. G., Pinkerton, M., Anderson, B., Thornhill, L.,
400 Hudgins, C., Winstead, E., Dibb, J. E., Scheuer, E., and Maring, H.: Results from the DC-8
401 Inlet Characterization Experiment (DICE): Airborne Versus Surface Sampling of Mineral
402 Dust and Sea Salt Aerosols, *Aerosol Sci. Tech.*, 41, 136-159,
403 <https://doi.org/10.1080/02786820601118406>, 2007.

404 Mgelwa, A. S., Song, L., Fan, M., Li, Z., Zhang, Y., Chang, Y., Pan, Y., Gurmesa, G. A., Liu, D.,
405 Huang, S., Qiu, Q., and Fang, Y.: Isotopic imprints of aerosol ammonium over the north
406 China plain, *Environ. Pollut.*, 315, 120376, <https://doi.org/10.1016/j.envpol.2022.120376>,
407 2022.

408 Noh, H.-j., Lee, S.-k., and Yu, J.-h.: Identifying Effective Fugitive Dust Control Measures for
409 Construction Projects in Korea, *Sustainability*, 10, 1206,
410 <https://doi.org/10.3390/su10041206>, 2018.

411 Park, S. H., Song, C. B., Kim, M. C., Kwon, S. B., and Lee, K. W.: Study on Size Distribution of
412 Total Aerosol and Water-Soluble Ions During an Asian Dust Storm Event at Jeju Island,
413 Korea, *Environ. Monit. Assess.*, 93, 157-183,
414 <https://doi.org/10.1023/B:EMAS.0000016805.04194.56>, 2004.

415 Philip, S., Martin, R. V., Snider, G., Weagle, C. L., van Donkelaar, A., Brauer, M., Henze, D. K.,
416 Klimont, Z., Venkataraman, C., and Guttikunda, S. K.: Anthropogenic fugitive, combustion
417 and industrial dust is a significant, underrepresented fine particulate matter source in global
418 atmospheric models, *Environ. Res. Lett.*, 12, 044018, [https://doi.org/10.1088/1748-](https://doi.org/10.1088/1748-9326/aa65a4)
419 [9326/aa65a4](https://doi.org/10.1088/1748-9326/aa65a4), 2017.

420 Qiu, H., Tian, L. W., Pun, V. C., Ho, K.-f., Wong, T. W., and Yu, I. T. S.: Coarse particulate
421 matter associated with increased risk of emergency hospital admissions for pneumonia in
422 Hong Kong, *Respiratory Epidemiology*, 69, 1027, [http://dx.doi.org/10.1136/thoraxjnl-2014-](http://dx.doi.org/10.1136/thoraxjnl-2014-205429)
423 [205429](http://dx.doi.org/10.1136/thoraxjnl-2014-205429), 2014.

424 Shah, V., Jacob, D. J., Moch, J. M., Wang, X., and Zhai, S.: Global modeling of cloud water
425 acidity, precipitation acidity, and acid inputs to ecosystems, *Atmos. Chem. Phys.*, 20, 12223-
426 12245, <https://doi.org/10.5194/acp-20-12223-2020>, 2020a.

427 Shah, V., Jacob, D. J., Li, K., Silvern, R. F., Zhai, S., Liu, M., Lin, J., and Zhang, Q.: Effect of
428 changing NO_x lifetime on the seasonality and long-term trends of satellite-observed
429 tropospheric NO₂ columns over China, *Atmos. Chem. Phys.*, 20, 1483-1495,
430 <https://doi.org/10.5194/acp-20-1483-2020>, 2020b.

431 Shao, Y. and Dong, C. H.: A review on East Asian dust storm climate, modelling and monitoring,
432 *Glob. Planet. Change*, 52, 1-22, <https://doi.org/10.1016/j.gloplacha.2006.02.011>, 2006.

433 Stelson, A. W. and Seinfeld, J. H.: Thermodynamic prediction of the water activity, NH₄NO₃
434 dissociation constant, density and refractive index for the NH₄NO₃-(NH₄)₂SO₄-H₂O system
435 at 25° C, *Atmos. Environ.*, 16, 2507-2514, [https://doi.org/10.1016/0004-6981\(82\)90142-1](https://doi.org/10.1016/0004-6981(82)90142-1),
436 1982.

- 437 Stone, E. A., Yoon, S.-C., and Schauer, J. J.: Chemical Characterization of Fine and Coarse
438 Particles in Gosan, Korea during Springtime Dust Events, *Aerosol Air Qual. Res.*, 11, 31-43,
439 <http://dx.doi.org/10.4209/aaqr.2010.08.0069>, 2011.
- 440 Tang, Y. and Han, G.: Characteristics of major elements and heavy metals in atmospheric dust in
441 Beijing, China, *J. Geochem. Explor.*, 176, 114-119,
442 <https://doi.org/10.1016/j.gexplo.2015.12.002>, 2017.
- 443 Tian, R., Ma, X., Sha, T., Pan, X., and Wang, Z.: Exploring dust heterogeneous chemistry over
444 China: Insights from field observation and GEOS-Chem simulation, *Sci. Total Environ.*,
445 798, 149307, <https://doi.org/10.1016/j.scitotenv.2021.149307>, 2021.
- 446 Travis, K. R., Crawford, J. H., Chen, G., Jordan, C. E., Nault, B. A., Kim, H., Jimenez, J. L.,
447 Campuzano-Jost, P., Dibb, J. E., Woo, J. H., Kim, Y., Zhai, S., Wang, X., McDuffie, E. E.,
448 Luo, G., Yu, F., Kim, S., Simpson, I. J., Blake, D. R., Chang, L., and Kim, M. J.: Limitations
449 in representation of physical processes prevent successful simulation of PM_{2.5} during
450 KORUS-AQ, *Atmos. Chem. Phys.*, 22, 7933-7958, [https://doi.org/10.5194/acp-22-7933-](https://doi.org/10.5194/acp-22-7933-2022)
451 [2022](https://doi.org/10.5194/acp-22-7933-2022), 2022.
- 452 Wang, X., Zhang, L., Yao, Z., Ai, S., Qian, Z., Wang, H., BeLue, R., Liu, T., Xiao, J., Li, X.,
453 Zeng, W., Ma, W., and Lin, H.: Ambient coarse particulate pollution and mortality in three
454 Chinese cities: Association and attributable mortality burden, *Sci. Total Environ.*, 628-629,
455 1037-1042, <https://doi.org/10.1016/j.scitotenv.2018.02.100>, 2018a.
- 456 Wang, Z., Pan, X., Uno, I., Chen, X., Yamamoto, S., Zheng, H., Li, J., and Wang, Z.: Importance
457 of mineral dust and anthropogenic pollutants mixing during a long-lasting high PM event
458 over East Asia, *Environ. Pollut.*, 234, 368-378, <https://doi.org/10.1016/j.envpol.2017.11.068>,
459 2018b.
- 460 Wang, Z., Pan, X., Uno, I., Li, J., Wang, Z., Chen, X., Fu, P., Yang, T., Kobayashi, H., Shimizu,
461 A., Sugimoto, N., and Yamamoto, S.: Significant impacts of heterogeneous reactions on the
462 chemical composition and mixing state of dust particles: A case study during dust events
463 over northern China, *Atmos. Environ.*, 159, 83-91,
464 <https://doi.org/10.1016/j.atmosenv.2017.03.044>, 2017.
- 465 Wesely, M. L.: Parameterization of surface resistances to gaseous dry deposition in regional-scale
466 numerical models, *Atmos. Environ.*, 23, 1293-1304, [https://doi.org/10.1016/0004-](https://doi.org/10.1016/0004-6981(89)90153-4)
467 [6981\(89\)90153-4](https://doi.org/10.1016/0004-6981(89)90153-4), 1989.
- 468 Wexler, A. S. and Seinfeld, J. H.: Analysis of aerosol ammonium nitrate: Departures from
469 equilibrium during SCAQS, *Atmos. Environ. Part A. General Topics*, 26, 579-591,
470 [https://doi.org/10.1016/0960-1686\(92\)90171-G](https://doi.org/10.1016/0960-1686(92)90171-G), 1992.
- 471 Woo, J.-H., Kim, Y., Kim, H.-K., Choi, K.-C., Eum, J.-H., Lee, J.-B., Lim, J.-H., Kim, J., and
472 Seong, M.: Development of the CREATE Inventory in Support of Integrated Climate and
473 Air Quality Modeling for Asia, *Sustainability*, 12, 7930,
474 <https://doi.org/10.3390/su12197930>, 2020.
- 475 Wu, Z., Zhang, X., and Wu, M.: Mitigating construction dust pollution: state of the art and the
476 way forward, *J. Clean. Prod.*, 112, 1658-1666, <https://doi.org/10.1016/j.jclepro.2015.01.015>,
477 2016.
- 478 Xing, J., Ye, K., Zuo, J., and Jiang, W.: Control Dust Pollution on Construction Sites: What
479 Governments Do in China?, *Sustainability*, 10, 2945, <https://doi.org/10.3390/su10082945>,
480 2018.

481 Xu, Q., Wang, S., Jiang, J., Bhattarai, N., Li, X., Chang, X., Qiu, X., Zheng, M., Hua, Y., and
482 Hao, J.: Nitrate dominates the chemical composition of PM_{2.5} during haze event in Beijing,
483 China, *Sci. Total Environ.*, 689, 1293-1303, <https://doi.org/10.1016/j.scitotenv.2019.06.294>,
484 2019.

485 Zhai, S., Jacob, D. J., Wang, X., Liu, Z., Wen, T., Shah, V., Li, K., Moch, J. M., Bates, K. H.,
486 Song, S., Shen, L., Zhang, Y., Luo, G., Yu, F., Sun, Y., Wang, L., Qi, M., Tao, J., Gui, K.,
487 Xu, H., Zhang, Q., Zhao, T., Wang, Y., Lee, H. C., Choi, H., and Liao, H.: Control of
488 particulate nitrate air pollution in China, *Nat. Geosci.*, 14, 389-395,
489 <https://doi.org/10.1038/s41561-021-00726-z>, 2021a.

490 Zhai, S., Jacob, D. J., Brewer, J. F., Li, K., Moch, J. M., Kim, J., Lee, S., Lim, H., Lee, H. C.,
491 Kuk, S. K., Park, R. J., Jeong, J. I., Wang, X., Liu, P., Luo, G., Yu, F., Meng, J., Martin, R.
492 V., Travis, K. R., Hair, J. W., Anderson, B. E., Dibb, J. E., Jimenez, J. L., Campuzano-Jost,
493 P., Nault, B. A., Woo, J. H., Kim, Y., Zhang, Q., and Liao, H.: Relating geostationary
494 satellite measurements of aerosol optical depth (AOD) over East Asia to fine particulate
495 matter (PM_{2.5}): insights from the KORUS-AQ aircraft campaign and GEOS-Chem model
496 simulations, *Atmos. Chem. Phys.*, 21, 16775-16791, [https://doi.org/10.5194/acp-21-16775-](https://doi.org/10.5194/acp-21-16775-2021)
497 [2021](https://doi.org/10.5194/acp-21-16775-2021), 2021b.

498 Zhang, Q., Shen, Z., Cao, J., Ho, K., Zhang, R., Bie, Z., Chang, H., and Liu, S.: Chemical profiles
499 of urban fugitive dust over Xi'an in the south margin of the Loess Plateau, China, *Atmos.*
500 *Pollut. Res.*, 5, 421-430, <https://doi.org/10.5094/APR.2014.049>, 2014.

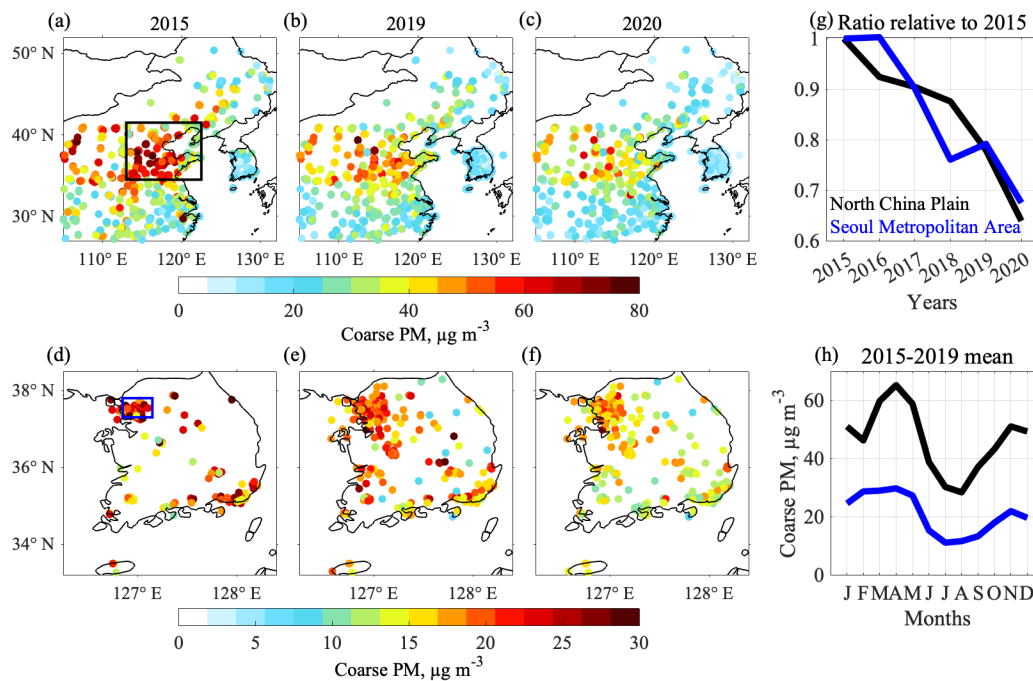
501 Zhao, G., Chen, Y., Hopke, P. K., Holsen, T. M., and Dhaniyala, S.: Characteristics of traffic-
502 induced fugitive dust from unpaved roads, *Aerosol Sci. Technol.*, 51, 1324-1331,
503 <https://doi.org/10.1080/02786826.2017.1347251>, 2017.

504 Zheng, B., Zhang, Q., Geng, G., Chen, C., Shi, Q., Cui, M., Lei, Y., and He, K.: Changes in
505 China's anthropogenic emissions and air quality during the COVID-19 pandemic in 2020,
506 *Earth Syst. Sci. Data*, 13, 2895-2907, <https://doi.org/10.5194/essd-13-2895-2021>, 2021a.

507 Zheng, B., Cheng, J., Geng, G., Wang, X., Li, M., Shi, Q., Qi, J., Lei, Y., Zhang, Q., and He, K.:
508 Mapping anthropogenic emissions in China at 1 km spatial resolution and its application in
509 air quality modeling, *Sci. Bull.*, 66, 612-620, <https://doi.org/10.1016/j.scib.2020.12.008>,
510 2021b.

511 Zheng, B., Tong, D., Li, M., Liu, F., Hong, C., Geng, G., Li, H., Li, X., Peng, L., Qi, J., Yan, L.,
512 Zhang, Y., Zhao, H., Zheng, Y., He, K., and Zhang, Q.: Trends in China's anthropogenic
513 emissions since 2010 as the consequence of clean air actions, *Atmos. Chem. Phys.*, 18,
514 14095-14111, <https://doi.org/10.5194/acp-18-14095-2018>, 2018.

515

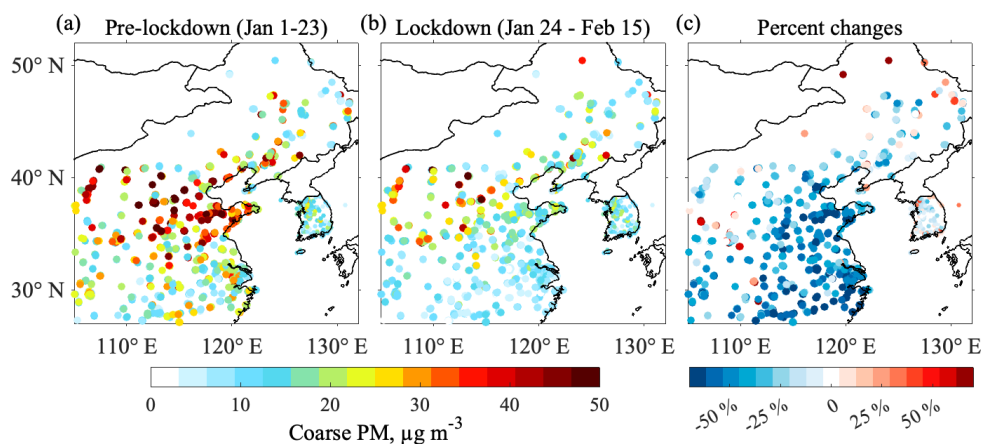


516

517

Figure 1. Distributions and trends of coarse PM concentrations over China and South Korea during 2015-2020. Here
 518 and elsewhere, coarse particulate matter (PM) is defined as particles between 2.5 and 10 μm aerodynamic diameter and
 519 its concentration is determined by subtracting $\text{PM}_{2.5}$ from PM_{10} in the air quality network data. Panels (a)-(c) show the
 520 annual mean concentrations in 2015, 2019, and 2020 over China and panels (d)-(f) show the same for South Korea. The
 521 rectangles in (a) and (d) delineate the North China Plain or NCP (113 - 122.5° E, 34.5 - 41.5° N) and the Seoul
 522 Metropolitan area or SMA (126.7 - 127.3° E, 37.3 - 37.8° N). Panel (g) shows annual trends relative to 2015 in the
 523 NCP (197 sites) and the SMA (33 sites) averaged over sites with at least 70% data coverage each year from 2015 to
 524 2020. Panel (h) shows the mean 2015-2019 seasonality over the NCP and SMA.

525

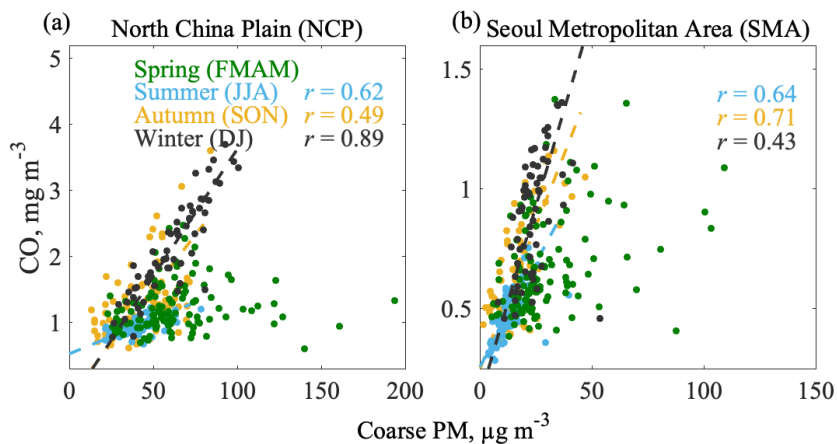


526

527 **Figure 2.** Response of coarse PM to COVID-19 lockdown in China. (a) Coarse PM averaged for the three weeks
 528 before the China national lockdown (January 1-23, 2020). (b) Coarse PM averaged during the three-week lockdown
 529 (January 24 - February 15, 2020). (c) Percent changes of coarse PM between lockdown and pre-lockdown periods.

530

531

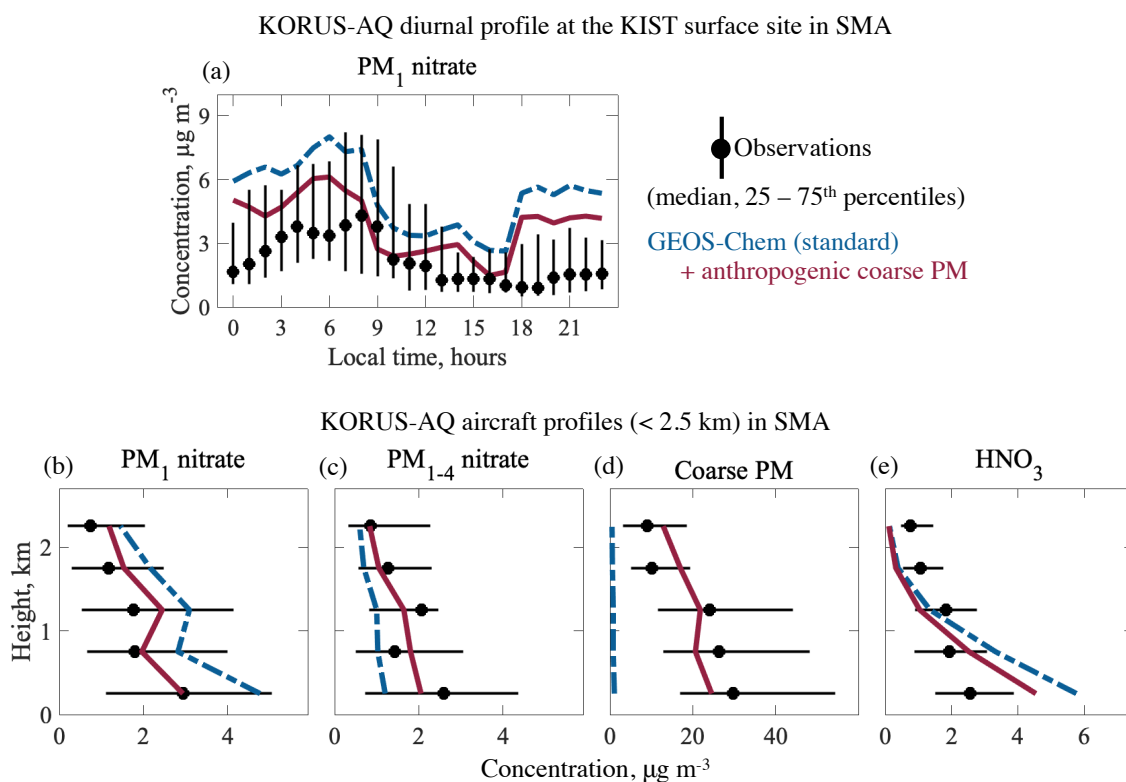


532

533 **Figure 3.** Daily correlations of coarse PM and CO concentrations over the North China Plain (NCP) and Seoul
 534 Metropolitan Area (SMA) in 2015. Coarse PM and CO concentrations are 24-h averages of air quality network
 535 observations spatially averaged over the two regions. Also shown are the correlation coefficients and reduced-major-
 536 axis regression lines except in spring when the correlation is not significant (p-value > 0.05). We include February in
 537 spring to cover the season of natural dust events (Tang and Han, 2017).

538

539



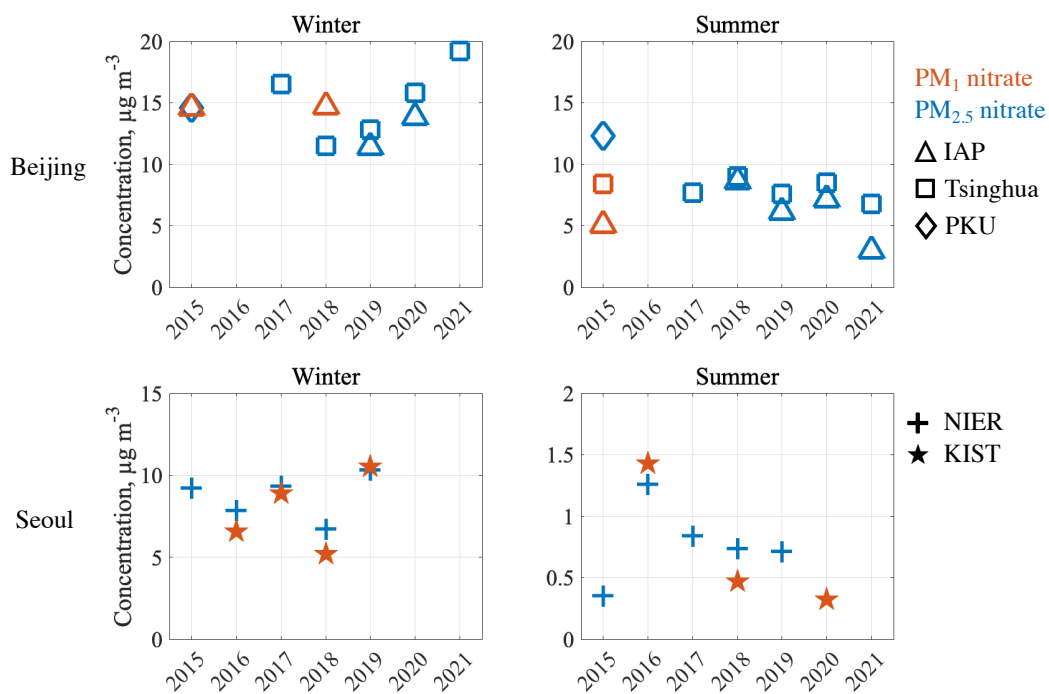
540

541 **Figure 4.** Effect of anthropogenic coarse PM on nitrate concentrations over the Seoul Metropolitan Area (SMA) during
 542 the KORUS-AQ campaign (May-June 2016). GEOS-Chem model results without (standard) and with anthropogenic
 543 coarse PM are compared to surface and aircraft observations. (a) Median diurnal variation (error bars are 25th and 75th
 544 percentiles) of non-refractory PM₁ nitrate (taken to be ammonium nitrate) at the Korea Institute of Science and
 545 Technology (KIST) site. (b)-(e) Median vertical profiles of non-refractory PM₁ nitrate, PM₁₋₄ nitrate, coarse PM (PM_{2.5-10}), and HNO₃
 546 concentrations for the ensemble of flights over the SMA. Horizontal bars for the observations indicate
 547 25th-75th percentiles.

548

549

Observed multi-year fine particulate nitrate in Beijing and Seoul

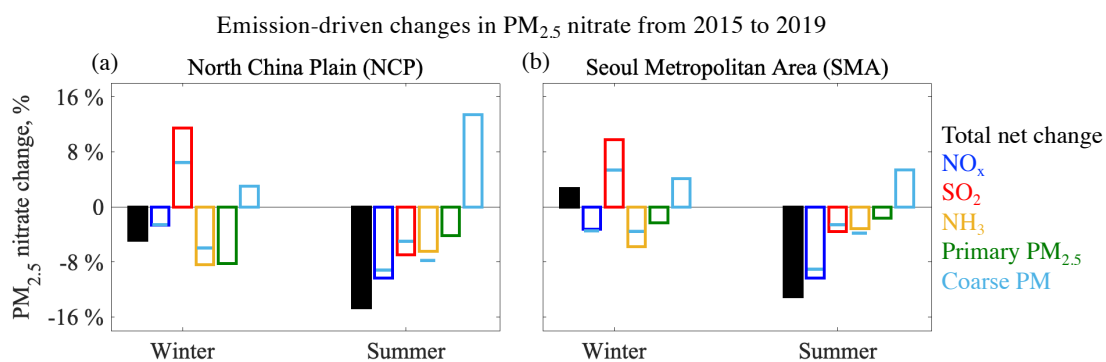


550

551 **Figure 5.** Long-term trend of fine particulate nitrate concentrations in Beijing and Seoul over the 2015-2021 period.
 552 Mean $\text{PM}_{1.0}$ or $\text{PM}_{2.5}$ concentrations in winter and summer are compiled from individual field campaigns in Beijing at
 553 the Institute of Atmospheric Physics (IAP), Tsinghua University (Tsinghua), and Peking University (PKU) sites and in
 554 Seoul at the National Institute of Environmental Research (NIER) and Korea Institute of Science and Technology
 555 (KIST) sites (Table S1). Note the differences in scales between panels.

556

557



Emission changes from 2015 to 2019

	NO _x	SO ₂	NH ₃	Primary PM _{2.5}	Coarse PM
NCP	-11%	-54%	-19%	-35%	-33%
SMA	-22%	-40%	0%	0%	-31%

558

559 **Figure 6.** Emission-driven changes in mean PM_{2.5} nitrate from 2015 to 2019 over the NCP and SMA. Results are from
 560 GEOS-Chem sensitivity simulations including total and individual emission changes over the period, all for the same
 561 meteorological year (2019) and applied both to China and South Korea (so the effects of NH₃ and primary PM_{2.5} over
 562 the SMA are due to long-range transport from China). Values are seasonal means for winter and summer. The blue
 563 lines superimposed on the NO_x, SO₂, and NH₃ sensitivity bars show the effects from simulations not accounting for the
 564 effect of HNO₃ uptake by anthropogenic coarse PM.

565